RSC Advances

PAPER

View Article Online
View Journal | View Issue

Cite this: *RSC Adv.*, 2024, **14**, 10662

Unveiling the multifaceted incorporation of *Musa acuminata* peduncle juice as a bio-corrosion inhibitor of mild steel in seawater-simulated solution

Abdelrahman Osama Ezzat,[a] Victor Sunday Aigbodion, *[bcd] Hamad A. Al-Lohedan[a] and Chinemerem Jerry Ozoude[e]

This work assessed the ability of *Musa acuminata* peduncle juice extract to sustainably inhibit mild steel under salinized conditions. The effort sought to ascertain the new active material's inhibitory efficacy for inhibiting metal corrosion in seawater. *M. acuminata* peduncle juice was extracted from the *M. acuminata* peduncle. The functional group of the *M. acuminata* pedal juice was determined using Fourier transform infrared spectroscopy. The corrosion behavior was assessed using electrochemical impedance spectroscopy and potentiodynamic polarization by varying the *M. acuminata* peduncle juice at 0.1, 0.2, and 0.3 g L^{-1} for 300 K, 310 K, and 320 K, respectively. Scanning electron microscopy provided an image of the surface morphology of mild steel. Reduced corrosion current (i_{corr}) was observed when *M. acuminata* pedal juice was present according to potentiodynamic polarization and studies. Moreover, adding *M. acuminata* peduncle juice increases resistance capacity transfer (R_{ct}). The potentiodynamic polarization approach was used to obtain the optimum inhibitory efficiency (%IE) at 0.3 g L^{-1} doses with 88.0% efficiency at 300 K. The addition of *M. acuminata* peduncle juice results in a smoother, mild steel morphology than the surface without inhibitor additions. The molecules of active chemicals adhering to the steel surface were linked to increased corrosion inhibition. The study's findings demonstrated that *M. acuminata* peduncle juice is a promising biomaterial for mild steel corrosion inhibitors in a salty environment.

Received 1st February 2024
Accepted 19th March 2024

DOI: 10.1039/d4ra00826j

rsc.li/rsc-advances

1 Introduction

Mild steel is apparently one of the most versatile metallic materials widely used in construction, manufacturing, marine, and diverse areas for other industrial and engineering purposes. However, the versatility of mild steel, and hence its engineering performance, is continually threatened because it is subject to corrosive environmental degradation.[1] One of the means to mitigate this destructive phenomenon, which can be disastrous and have economic and technological consequences, is the use of chemical inhibitors.[2] These chemical compounds are adsorbed on metal surfaces to minimise, control, and/or prevent corrosion-destructive processes and reactions. The use of chemical inhibitors to decrease the rate of corrosion processes is quite varied. In the marine environment and processing industries, inhibitors have always been considered the first line of defense against corrosion.[3–5] However, scientists prioritise inhibitor types derived from natural or organic sources. This substance was selected due to its great availability, low toxicity, and ease of acquisition as a result of its plentiful natural availability. Many natural compounds such as those found in terebinth,[6] watermelon,[7] nettle leaves,[8] tomato pomace,[9] piper guineense,[10] unripe banana peel extract,[11] starch and cellulose,[12] and *Musa acuminata* inflorescence[13] are used to reduce mild steel from corrosion in salt water.

The economical, logical, and scientific presentation of data is an aspect that must be considered when using plant extracts as green materials for corrosion inhibitors. To make the process more effective and efficient, a methodical and strategic strategy for using green material inhibitors is logically and rationally advised. In this work, mild steel was exposed to a simulated saltwater environment using an artificial seawater solution because oil pipelines are frequently subject to corrosion in seawater, and *Musa acuminata* peduncle juice is employed as

[a]*Department of Chemistry, College of Sciences, King Saud University, Riyadh 11451, Saudi Arabia*
[b]*Faculty of Engineering and the Built Environment, University of Johannesburg, P. O. Box 534, Auckland Park, South Africa*
[c]*Department of Metallurgical and Materials Engineering, University of Nigeria, Nsukka Postal Code 410001, Nigeria*
[d]*Africa Centre of Excellence, ACESPED University of Nigeria, Nsukka Postal Code 410001, Nigeria*
[e]*Department: Materials Science and Engineering, University of North Texas, Denton, Texas, USA. E-mail: victor.aigbodion@unn.edu.ng*

corrosion inhibition. This *Musa acuminata* peduncle juice extract can be used to solve the mild steel corrosion problem in seawater and the associated issues in several scenarios. Additionally, it is worth mentioning that *Musa acuminata* peduncle juice has high amounts of several bioactive substances,[14] helps make biodiesel,[15] and has healing properties,[16] to name a few. However, there is little or no information on the inhibition properties and potential of *M. acuminata* peduncle juice on mild steel. This work reports for the first time the corrosion inhibitor behaviour of mild steel in *M. acuminata* peduncle juice (MAPJ) and contributes to knowledge in this direction of material development. MAPJ was chosen for this work because it was reported by ref. 17 that MAPJ contains bioactive and inhibition properties, such as 21.20% *cis*-9-hexadecenal, 18.81% pentadecanoic acid, 16.04% benzoic acid, 6.18% octadecanoic acid, and 22.24% pyrogallol, as evidenced by their GS-MS analysis.

2 Materials and methods

2.1. Materials

Table 1 shows the composition of the mild steel API 5 L pipeline sample used in this research, which was obtained from the Nigeria National Petroleum Company, Warri, Nigeria. The sample was formed into a working electrode by cutting it into dimensions of 1 cm by 1 cm. The high-salinity solution was made using artificial seawater in accordance with ASTM D 1141. *M. acuminata* peduncle was acquired from the University of Nigeria Nsukka Farm (see Fig. 1).

2.2. *M. acuminata* peduncle juice (MAPJ) preparation

The *M. acuminata* peduncles were cleaned and rinsed and then their green outer layer was peeled off, chopped into little pieces, and baked at 65 °C. The juice was extracted using a process of mechanical crushing made of Retsch Planetary Ball Mill PM 400 and filtered through a muslin cloth to obtain *M. acuminata* peduncle juice. The Shimadzu Fourier Transform Infrared (FT-IR) model, IRTracer-100, was used to characterise the MAPJ. To prepare the combination for FTIR spectroscopy, 250 mL of MAPJ is mixed with KBr to develop a palette. The analysis was performed in the 4000–500 cm^{-1} wave number range.

2.3. Preparing mild steel

The process of obtaining mild steel samples involves cutting API 5 L pipes. Each test coupon has dimensions of 1 cm by 1 cm, so the area is one cm^2 in total. Diepoxy and a current-connecting wire were used to join the sides. Abrasion was applied to the samples using metallurgical grit papers of grades 120 to 1200. In addition, the samples were cleaned using ethanol and then dried using hot air to get ready for use in corrosion research.

Fig. 1 Photograph of *Musa acuminata* Peduncle.

2.4. Measuring electrochemical reactions

The corrosion behaviour was determined using electrochemical measurements performed using a model CHI660D electrochemical device. A traditional three-electrode electrochemical cell was used in the studies. A 1 cm^2 mild steel specimen served as the working electrode. The reference electrode was an AgCl electrode, while the counter electrode was a graphite electrode. The electrodes were immersed in a 250 mL beaker containing the simulated sea water and inhibitor of MAPJ at 0.1, 0.2, and 0.3 g L^{-1}. After 400 seconds of recording open circuit potential (OCP) data, the amount of time required for OCP to approach a quasi-stationary state. Polarization measurements were made at a scan rate of 0.5 mV s^{-1} for 300, 310, and 320 K. The investigations on polarisation and impedance were conducted using a 30 minutes immersion duration. Tafel plots were used to compute the electrochemical parameters, such as corrosion potential (E_{corr}), corrosion current density (i_{corr}), and corrosion rate. For the electrochemical impedance spectroscopy (EIS) method, a 10 mV small-amplitude AC signal with a frequency ranging from 0.1 Hz to 0.5 MHz was impressed at the OCP. The impedance data were then examined using Nyquist plots. An analysis was performed on the parameters derived from the equivalent circuit that suited the best. Chem Anlyts software was used to evaluate the curves, and the formulae in ref. 18 and 19 were used to calculate the polarisation resistance and inhibitory efficiency:

$$R_P = \frac{\beta_a \beta_c}{2.3 i_{corr}(\beta_a + \beta_c)} \quad (1)$$

$$\%\ IE = \frac{(\text{corr. rate})_0 - (\text{corr. rate})_i}{(\text{corr. rate})_0} \quad (2)$$

where β_c and β_a, are the cathodic and anodic and Tafel constants and i_{corr} (current density), respectively. The inhibited specimen's corrosion rate is represented as (corr. rate) i, and the control sample corrosion rate is indicated as (corr. rate).

Table 1 Elemental composition of carbon steel is used in this work

Element	C	Mn	Si	P	S	Cr	Mo	Ni	Ti	Fe
Amount (wt%)	0.111	2.09	0.307	0.180	0.085	0.020	0.0045	0.0056	0.054	Balance

2.5. Examination of the surface

A highly effective method for examining the alterations introduced by corrosion on the electrode surface is surface analysis. A VEGA 3 TESCAN scanning electron microscope was used to examine the surface of the samples.

3 Results and discussion

3.1. FTIR analysis

FTIR analysis was used to examine the inhibitor layer's composition that was adsorbed on the steel surface. The FT-IR spectra of several samples are shown in Fig. 2. FTIR analysis was used to examine MAPJ adsorption on the surface of mild steel in the presence of 0.3 g L^{-1}. The prominent absorption band at 3600 cm^{-1} confirms the existence of OH groups, and the C–H sharp quadrant stretch of the alkane medium was observed at an absorption of 1501 cm^{-1}. Ester and carbonyl C═O,═C–H generally strong stretch functional groups at wave number 2208. 5 cm^{-1}. The C–O extension of an aromatic alcohol was obtained at a band of 1044 cm^{-1}. The frequency of the bands caused by the aromatic OH bands depends on the replacement of the aromatic rings. The extract is believed to contain biomolecules with advantageous qualities for corrosion inhibition based on the FTIR spectra analysis and is also in line with the structure of MAPJ. The FTIR absorption bands showed slight changes according to the results. The sample exposed to 0.3 g L^{-1-1} MAPJ showed a shift in higher peaks compared to the MAPJ. This confirmed that the MAPJ was absorbed on the mild steel surface. The adsorption of several MAPJ components on the surface of mild steel is shown in the changes above. Therefore, the interaction of the inhibitor on the mild steel surface is shown by the FT-IR spectra investigations.[12] These band shifts verify that the green inhibitor interacts with the metal surface physically and chemically.

3.2. Open circuit potential (OCP)

The OCP value changes when an inhibitor is present are often helpful in determining whether cathodic or anodic reactions are the most impacted. Fig. 3 shows that for the first 400 seconds at room temperature, the OCP of the inhibition sample shows a positive voltage shift compared to the OCP of the blank solution. This positive change in the OCP when MAPJ is present suggests that MAPJ affects the mild steel corrosion anodic response. According to this first finding, MAPJ may be able to slow down anodic processes, such as the oxidation of mild steel surfaces, when there is an open circuit. This is consistent with several studies.[20,21]

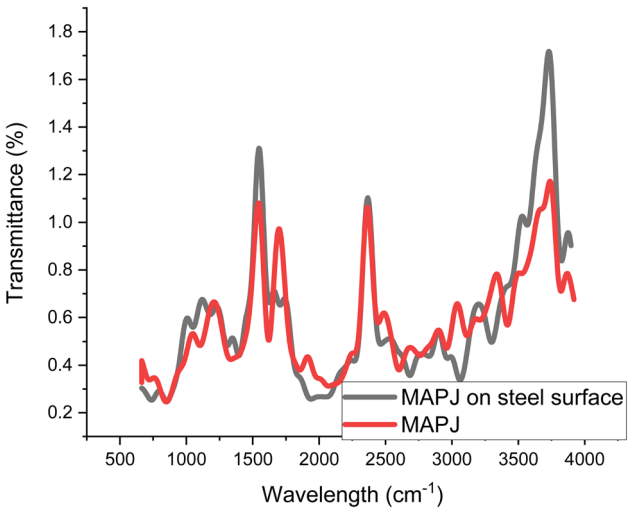

Fig. 2 FTIR analysis of the MAPJ.

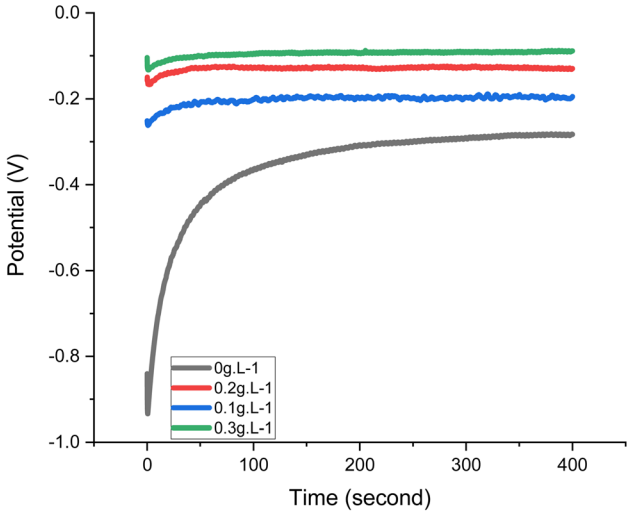

Fig. 3 OCP curves of the mild steel with and without MAPJ at 300 K.

3.3. Potentiodynamic polarisation

The corrosion current density (i_{corr}), which was lower in the inhibited samples, is shown in Fig. 4. This measurement's outcome demonstrated that mild steel corrodes less when the concentration of extract increases. Values for E_{corr} and i_{corr} were obtained by fitting curves after Echem Analyst software was put into use. There is an electrochemical corrosion potential (E_{corr}) that changes strength in both the positive (anodic) and negative (cathodic) directions of the mild steel sample. According to ref. 18, this discovery suggests that the material is isolated from MAPJ functions as a mixed-type inhibitor. It is commonly acknowledged that i_{corr} functions as a direct measure of corrosion rate. Furthermore, as Fig. 4 illustrates, the corrosion current (i_{corr}) dropped as the extract concentration rose and finally reached a minimum value of 0.3 g L^{-1}. Specifically, as the extract concentration increases, the i_{corr} decreases, so the corrosion rate also decreases. This study's results align with previous findings, which showed that the corrosion current decreased as the inhibitor concentration increased[21] and supported the results of the OCP above.

The results showed that a greater inhibition efficiency of 88.0% was obtained at an extract concentration of 0.3 g L^{-1}. The potentiodynamic curve demonstrates that MAPJ slows steel corrosion in a saline solution with roughly 3.5% NaCl. One way that the current invention works is that biomolecules made from heteroatoms adsorb to the surface of mild steel or low-carbon steel and block the active corrosion zones there.[21] Table 2 shows the electrochemical parameters found by

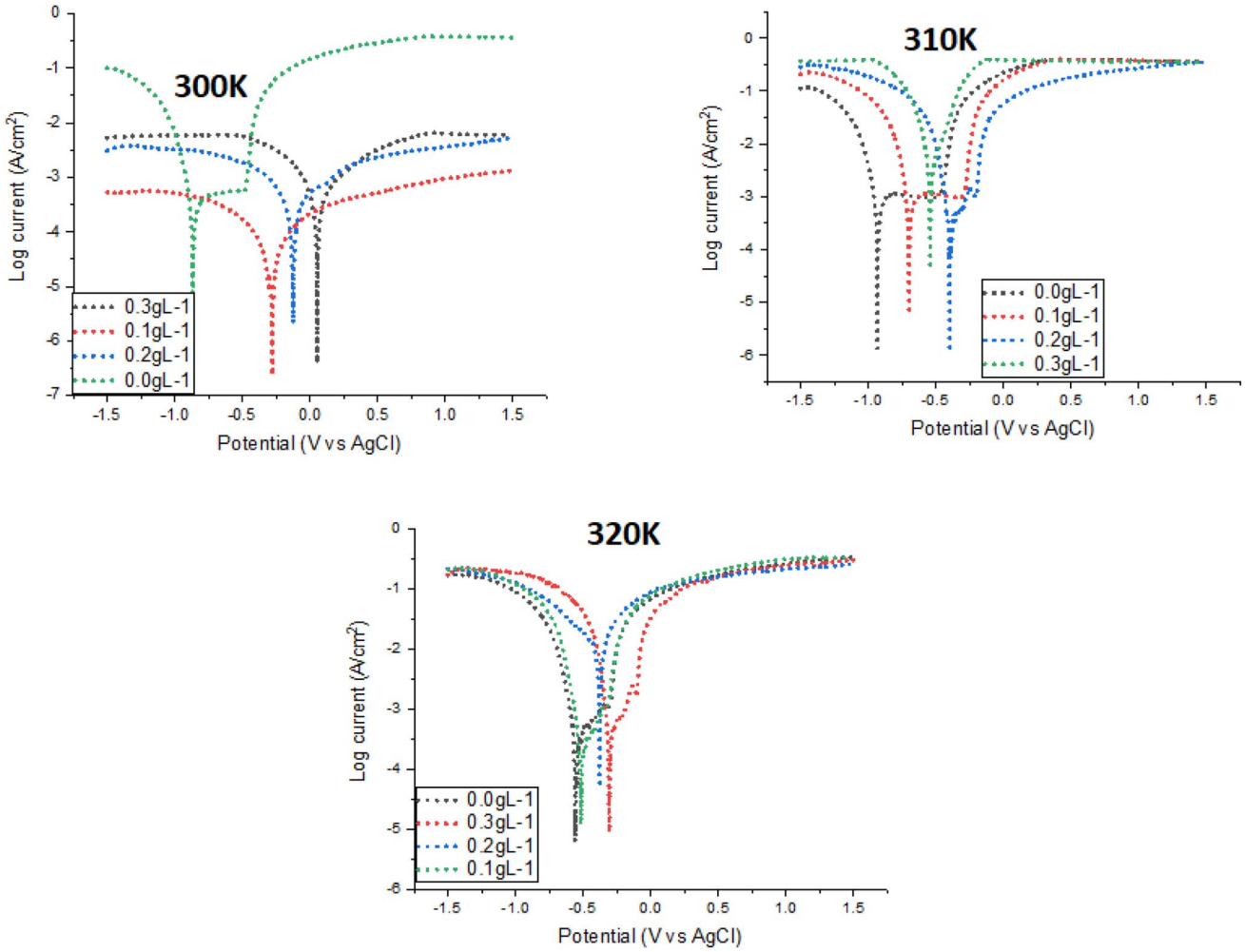

Fig. 4 Potentiodynamic polarization curves of mild steel with and without MAPJ extracts at different temperatures in saline environments.

analysing the polarisation curve. These include the corrosion current (i_{corr}), the polarisation resistance, and the corrosion potential (E_{corr}). The effect of adding the extract while reducing the corrosion rate and increasing the inhibition efficiency (%IE) is visible. The inhibition efficiency value is calculated based on a comparison of corrosion current data with and without the addition of extract. The addition of an inhibitor slows down the generation of hydrogen while simultaneously reducing iron dissolution.[22] From Table 2, we saw that the anodic polarisation changed as the temperature increased from 300 to 320 K and increased in plant extract content. This suggests that double layer capacity decreases and mass transfer increases in the presence of increased inhibitor concentrations. A decrease in the rate of carbon steel dissolving results in an increase in the % IE values with larger surface coverage. It is evident from the above that the plant extracts created a coating that protected the carbon steel's surface. Additionally, increasing the temperature causes the %IE to reduce. This indicates that inhibitor molecules are less adsorbed and do not function well as inhibitors on the anodic sites as the temperature increases.

The concentration of MAPJ causes an increase in surface covering. As the concentration of the inhibitors increases, the current density and corrosion rate values decrease. This shows that a barrier layer forms on the surface of the mild steel. Due to electrostatic interactions, this enables the protonated extract to physically adsorb onto the surface of the charged carbon steel, boosting its protective effect. Partial electron transfer on the tested carbon steel surface allows the adsorbed protonated components of plant extracts to be coordinated during chemical adsorption. Lone pairs from their oxygen and nitrogen atoms occupy empty carbon steel d-orbits, or they may combine with newly produced Fe ions at the metal surface to create metal-inhibitor complexes that might adsorb to an electrode across van der Waals forces, preventing carbon steel from corroding. This confirms that the carbon steel's physicochemical adsorption type was inferred from adsorption isotherm calculations.[23,24]

3.4. Electrochemical impedance spectroscopy (EIS)

Experiments utilizing EIS are commonly used to examine and delineate corrosion processes occurring on diverse metal surfaces. Using the equivalent circuit (Fig. 5) to analyse the EIS spectra, a single charge transfer process was found. The addition of MAPJ extract enhanced the diameter of the capacitance

Table 2 Electrochemical parameters of the potentiodynamic polarization of API 5 L steel in synthetic seawater media

MAPJ (g L^{-1})	I_{corr} (A cm^{-2})	E_{corr} (V)	Polarisation resistance (ohm)	Corrosion rate (MPY)	θ	IE %
300 K						
0	1.57×10^{-2}	−0.81	2	14.37	0	0
0.1	5.045×10^{-4}	−0.45	94	4.618	0.680	0.68
0.2	2.605×10^{-4}	−0.40	178	2.385	0.830	83.0
0.3	1.91×10^{-4}	−0.35	249	1.751	0.880	88.0
310 K						
0	1.69×10^{-2}	−0.87	3	15.47	0	0
0.1	5.181×10^{-4}	−0.55	86	4.743	0.662	66.2
0.2	2.823×10^{-4}	−0.50	165	2.58	0.811	81.1
0.3	2.159×10^{-4}	−0.51	217	1.976	0.872	87.2
320 K						
0	2.39×10^{-2}	−0.86	2	21.88	0	0
0.1	2.364×10^{-4}	−0.56	141	8.41	0.615	61.5
0.2	3.797×10^{-4}	−0.52	140	6.48	0.704	70.4
0.3	2.490×10^{-4}	−0.50	188	4.27	0.805	80.5

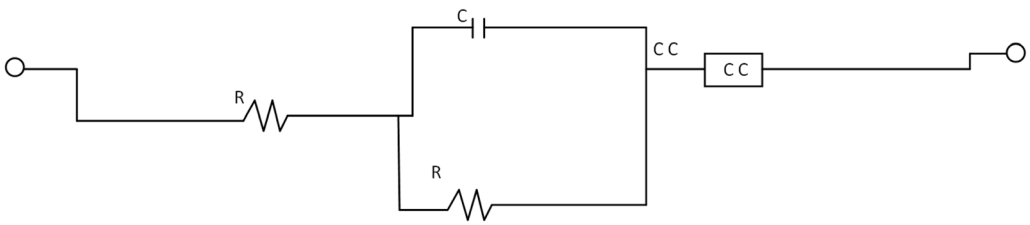

Fig. 5 A circuit model was used to analyze the performance of MAPJ extract as in seawater media.

loop produced in the simulated seawater solution, showing corrosion inhibition behaviour. The R values with the MAPJ inhibitor are consistent with the outcomes of the polarisation strategy. The Nyquist and Bode phase curves of mild steel in a saline solution, without MAPJ and 0.3 g L^{-1} MAPJ, are shown in Fig. 6 and 7. The Nyquist curve displays a distinctive depressed semicircle pattern, with a positive association between the semicircle's diameter and the amount of extract applied. These results are consistent with those of previous studies[23,24] (Fig. 6). This assertion is substantially supported by the data in ref. 24, which shows the Bode phase angle (Fig. 7).

The Bode phase angle also showed mild steel corrosion and corrosion inhibition in the saline solution, suggesting that the electrolyte and steel surface had only one interface. A protective layer covering the steel's surface made of biomolecules from MAPJ could be the reason for this outcome. The presence of

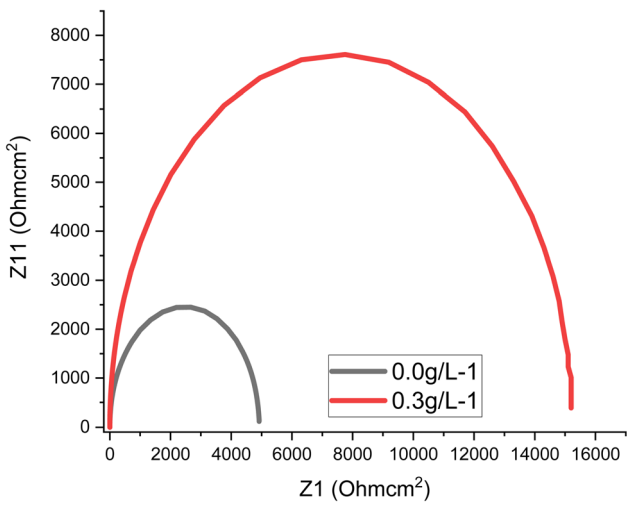

Fig. 6 Results of Nyquist curve for API 5 L steel with and without MAPJ extract based on synthetic seawater.

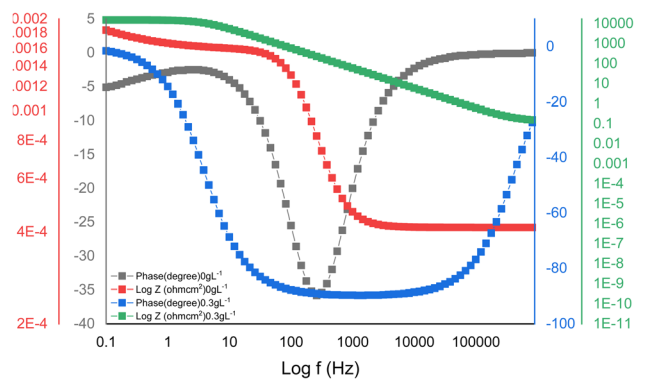

Fig. 7 Bode curve results for API 5 L steel with and without MAPJ extract-based synthetic seawater.

inhibitor decreases the CC values, while the R values increase, *e.g.*, values of 60.5 and 10.8 μF cm^2 and 5000 and 14500 Ωm were recorded for the CC and R, respectively. Reduced values are associated with either an increase in protective layer thickness or a decrease in the local dielectric constant. The growth of an inhibitive layer on the surface of mild steel is shown by the capacitive loop widths becoming wider in the Nyquist plots.[25]

3.5. Mechanism of adsorption

To better understand how MAPJ inhibits corrosion on mild steel in saline settings, this study investigates the adsorption behavior of MAPJ on the surface of the steel. For this analysis, the data shown in Table 2 are utilized. The experimental data were found to agree with the Freundlich isotherm (eqn (3) and (4)).[24] Fig. 8 shows the results of the concentration plotting and surface coverage (θ). The adsorption equilibrium constant (K_{ads}) was calculated using the straight-line fitting intersection approach. The values obtained from the Freundlich isotherm are positive; this demonstrates that positive values of the adsorption parameter indicate the inhibitor's appealing behavior on the mild steel surface.[25] The adsorption efficiency of MAPJ increases at lower temperatures and decreases at higher temperatures according to the K_{ads} value, which shows a positive association with temperature. Eqn (5), as mentioned in ref. 25, is used to simultaneously determine free energy adsorption (ΔG_{ads}):

$$\mathrm{Log}\,\theta = \mathrm{Log}\,C + \mathrm{Log}\,K \tag{3}$$

$$\theta = \frac{\eta}{100} \tag{4}$$

$$\Delta G_{ads} = -2.393RT\,\mathrm{Log}(10^3 K_{ads}) \tag{5}$$

$$\Delta G = \Delta H - T\Delta S \tag{6}$$

In this instance, the variables T and R represent the Kelvin (K) process temperature and the joules per milliliter per Kelvin (J mL^{-1}. K^{-1}) gas constant, respectively. High K_{ads} and low G_{ad} values frequently indicate that inhibitor elements are effectively adsorbed onto the metal surface. The adsorption process entropy (ΔS) and adsorption enthalpy (ΔH) can be found in relation to the free energy (ΔG) using the Van der Hoff equation, as illustrated below (eqn (6)).[25] The results of fitting the natural are shown in Fig. 8, where a straight line is obtained. These numbers were used in the computation that was performed to determine the values of ΔH_{ads} and ΔS_{ads}.

Values of 2.4, 1.9 and 1.6 (10^5 M^{-1}) were obtained for K_{ads}. It is evident that when temperature increases, K_{ads} values decrease. This finding suggests that the metal surface is physically adsorbed by the inhibitor. The molecules of the adsorbent have modest forces of attraction when there is physical adsorption. Through charge sharing or charge transfer from the inhibitor molecules to the metal surface, the adsorbate molecules and the adsorbent molecules or atoms present on the surface create chemical interactions that take the form of coordinate-type bonds.[24] The high K_{ads} values imply a strong

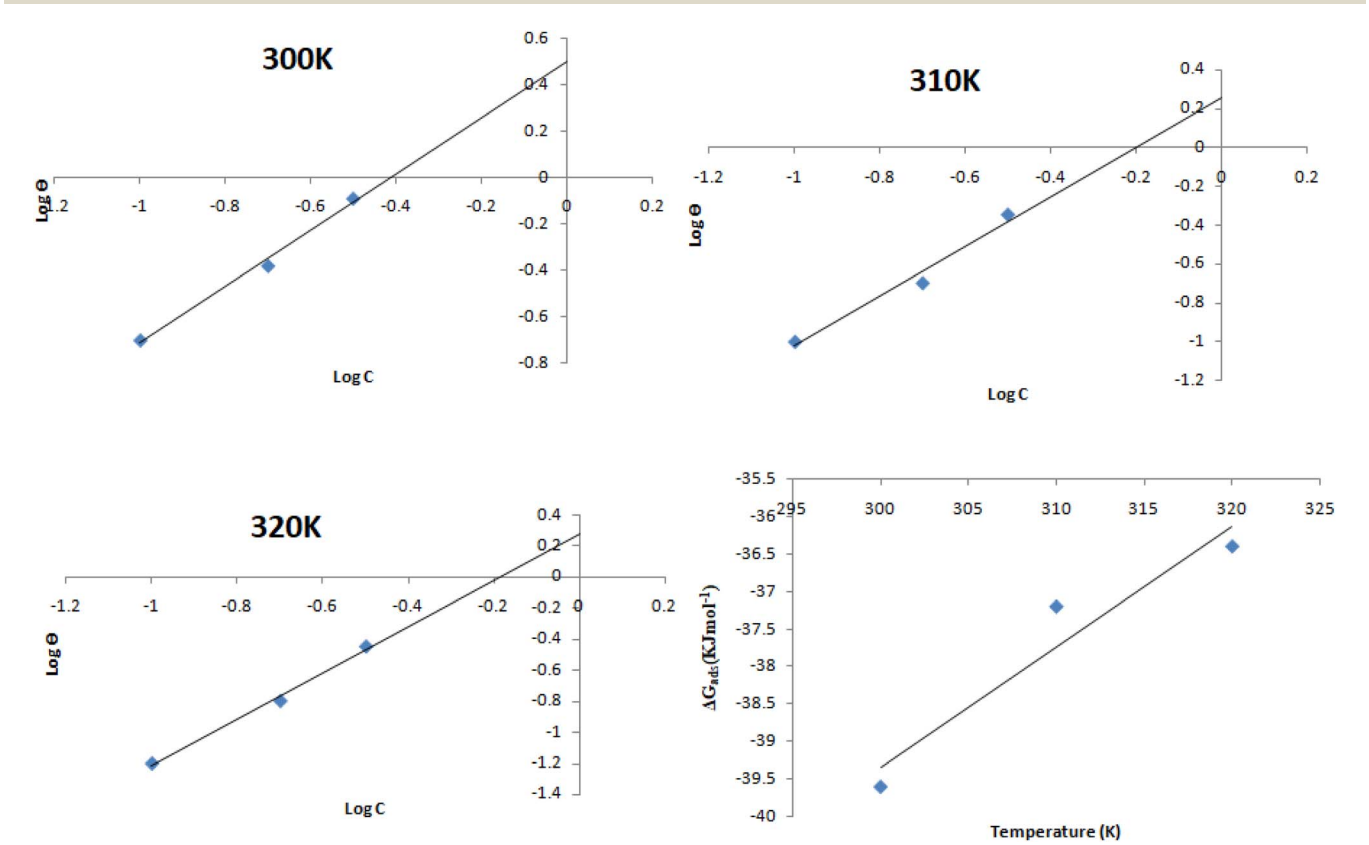

Fig. 8 Curve diagrams of Freundlich isothermal and free energy with temperature.

connection between the adsorbed molecules and the metal surface, meaning that the inhibitor molecules are difficult for the solvent molecules to remove from the surface.

The calculated values of ΔG_{ads} are −39.6, 37.2 and −36.4 kJ mol^{-1}. These results indicate that the adsorption mechanism of MPJ on mild steel in simulated seawater solution is typical of physisorption at the studied temperatures. Generally, absolute values of ΔG_{ads} of the order of −40 kJ mol^{-1} indicate chemisorptions. The high negative values obtained for ΔG_{ads} indicate that the adsorption process occurs spontaneously by strong interactions between the steel surface and inhibitor, as was suggested by the obtained values of K_{ads}. Thermodynamically, ΔG_{ads} is related to the entropy and enthalpy of the adsorption process, ΔH_{ads} and ΔS_{ads}, respectively, as illustrated in eqn (6).

In Fig. 9, the plot of ΔG_{ads} ads *vs.* T gives a straight line with an intercept of ΔH_{ads} and a slope of ΔS_{ads}.[23] Adsorption is generally accompanied by the release of energy, that is, most adsorption processes are exothermic in nature. An endothermic adsorption process ($\Delta H_{ads} > 0$) signifies unequivocal chemisorption, while an exothermic adsorption process ($\Delta H_{ads} < 0$) may involve either physisorption or chemisorption or a mixture of both processes.[2,18] The obtained values of ΔH_{ads} and ΔS_{ads} are −42.2 kJ mol^{-1} and −21.2 J K^{-1} mol^{-1}, respectively. The ΔH_{ads} value in the presence of the MPJ inhibitor is highly negative, indicating that the adsorption of the inhibitor molecules onto the metal surface is an exothermic process. In the present study, the ΔH_{ads} value is larger than the expected physical adsorption but smaller than the one for chemical adsorption. This result suggests that the adsorption mechanism of MPJ on mild steel in simulated seawater at the studied temperatures could involve both physisorption and chemisorption at different concentrations. The obtained negative value of ΔS_{ads} indicates a reduction in translational degrees of freedom. This means that an increase in order occurs when moving from the free bulky inhibitor molecules is chaotic to the more orderly inhibitor molecules on the metal surface.

3.6. Corrosion mechanism

Three distinct stages, initiation, propagation, and termination, can be used to explain the sequential advancement of pitting formation and the corrosive reaction of steel in a saline environment. A chemical reaction facilitates the dissolution of the metal, which breaks down the passive layer in the anodic region and starts the initiation process.[26–28] Within the cathodic region, an oxygen-related reaction occurs *via* the mechanism of the degree of coverage. Eqn (7)–(9) can be used to express the total reactions as follows:

$$Fe = Fe^{2+} + e^{-} \quad (7)$$

$$O_2 + 2H_2O + 4e^{-} = 4OH^{-} \quad (8)$$

$$4Fe + O_2 + 2H_2O = 4Fe(OH)_2 \quad (9)$$

The anodic area becomes overly concentrated with positive Fe^{2+} ions due to the continuous dissolving of the metal. Simultaneously, Cl^{-} ions exit the electrolyte to maintain charge

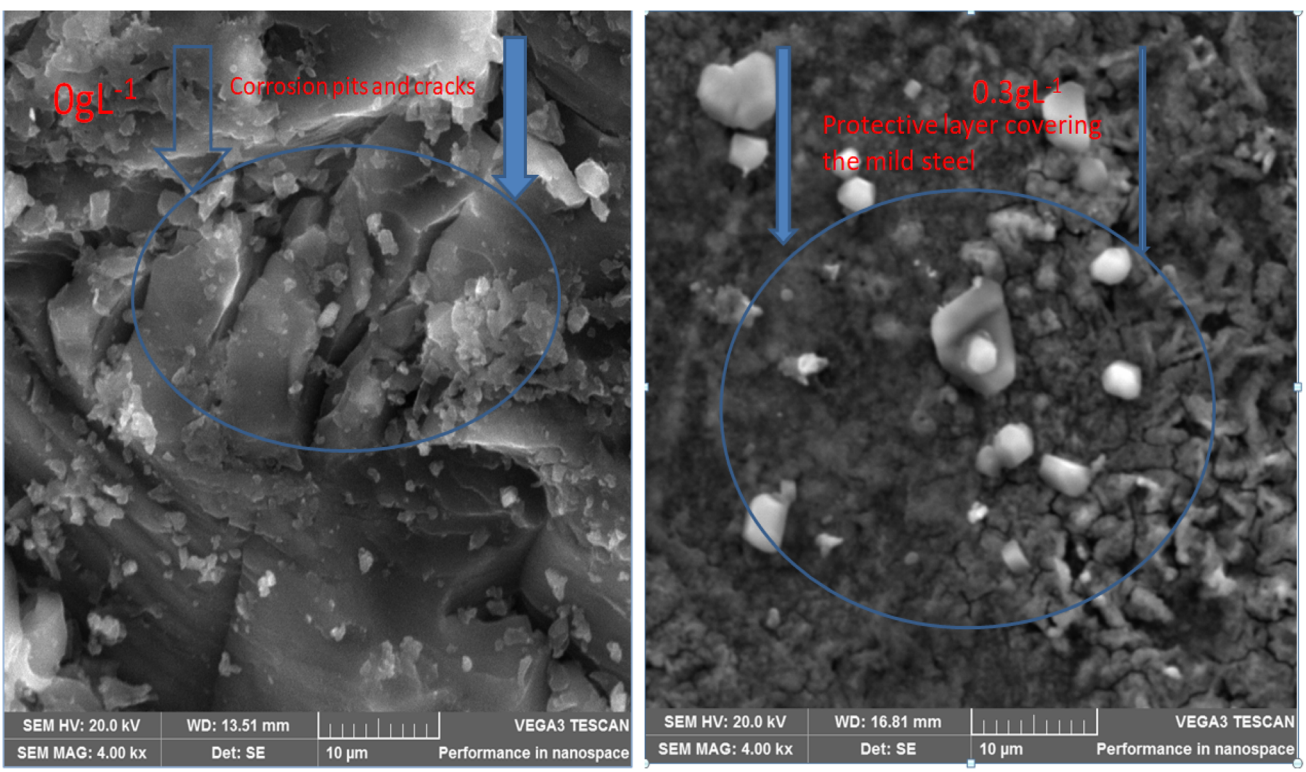

Fig. 9 SEM images of the corroded samples at 0 and 0.3 g L^{-1}.

neutrality. Eqn (10) shows that iron and this negative ion (Cl^-) react to form ferric chloride:

$$Fe^{2+} + Cl^- = FeCl \quad (10)$$

Eqn (11) illustrates the interaction between FeCl and H_2O, which produces FeOH, H^+, and Cl^-ions. The presence of both H^+ and chloride ions inhibits the repassivation process. FeCl is produced at a higher rate when the anode disintegrates faster because it increases the pace at which chloride ions migrate. The aforementioned procedure keeps going until the metal causes a hole to appear. This phenomenon is known as the autocatalytic process, and it shows gradual expansion over time, leading to an increase in metal degradation and the creation of metal holes.

$$FeCl + H_2O = FeOH + H^+ + Cl^- \quad (11)$$

3.7. SEM images of corroded surfaces

The corroded surfaces of the mild steel surfaces are shown in Fig. 9 using a scanning electron microscopy (SEM) image. It is clearly observed that the 0 g L^{-1} MAPJ has much more flaws and uneven surfaces than mild steel inhibited with the 0.3 g L^{-1} MAPJ. In the inhibited sample, the passive layer covered the steel surface as a result of the inhibition effect of the MAPJ, which helped delay and reduce the rate of reaction between the mild steel and the simulated seawater environment. This observation suggests that MAPJ can effectively inhibit mild steel in saline solutions containing NaCl. The study's findings unequivocally demonstrate that mild steel corrodes significantly in NaCl in the absence of MAPJ. However, MAPJ significantly lessened the negative impact of NaCl on the mild steel surface.

3.8. Molecular dynamics simulations (MD)

This technique is a well-established tool in computational chemistry and can be used to uncover hidden factors that can aid in understanding and characterising the adsorption performance of the inhibitor plant extract molecules on the surface of carbon steel as well as the interactive forces of the tested inhibitor. Because several organic compounds were chosen from the GC/MS data based on their greatest percentage recorded in the plant extract,[17] it is believed that they are the cause of the highest inhibition rate and were used for the MD. The determination of the lowest energy adsorption sites for molecular adsorbates on Fe (001) surfaces was conducted by utilizing the adsorption locator module in the Materials Studio suite of code. This module employs a Monte Carlo algorithm to thoroughly explore the entire configurational space of adsorbate–surface interactions. It considers multiple degrees of freedom, encompassing rotations and translations of the adsorbate on the surface. The primary objective is to assess and identify configurations with the lowest energy levels. This module, employed in numerous studies, facilitated the assessment of the lowest energy surface–adsorbate configuration (SAC). To ascertain the optimal SAC, molecular adsorbates were pre-adsorbed, allowing for the identification of the configuration with the lowest energy. Fig. 10 illustrates the structure of the Fe (001) surface with adsorbates on the surface. The goal of the adsorption calculation was to identify the minimum energy state for the entire system. Table 3 displays various outputs and descriptors, including the total energy of the substrate–adsorbate configuration in kcal mol^{-1}. This total energy encompasses the sum of the adsorbed component energies, rigid adsorption energy, and energy deformation. In this investigation, adsorption energy (kcal mol^{-1}) represents the released or required energy when the relaxed adsorbate components adhere to the substrate. Tabulated data also include (dE_{ads}/dNi), indicating the energy of substrate–adsorbate configurations (in kcal mol^{-1}) when one of the adsorbate components is removed. Table 3 provides insights into the interaction energy (E interaction) and binding energy (E binding) values between the natural organic components in the studied plant extracts and the Fe (110) surface, particularly when systems reach equilibrium. The findings reveal that the interaction energy ($-E$ binding) for all the studied inhibitors carries a negative value, suggesting the spontaneous adsorption of natural organic constituents on the Fe (110) surface. Notably, higher adsorption energy values indicate that selected molecules of natural organic constituents exhibit superior efficiency in inhibition.

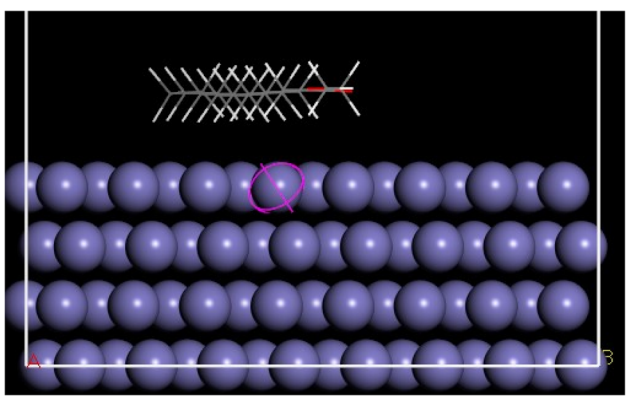

Fig. 10 Molecular dynamics simulation of the process.

Table 3 Results from the molecular dynamics simulation

Total energy kcal mol^{-1}	Adsorption energy kcal mol^{-1}	Rigid adsorption energy kcal mol^{-1}	Deformation energy kcal mol^{-1}	dE_{ad}/dNi	Binding energy kcal mol^{-1}
−55.651	−65.062	−51.200	−13.173	−65.062	−65.062

4 Conclusions

Musa acuminata peduncle juice, a new inhibitor of the biocorrosion of mild steel in a saline environment, was investigated in this study. It was concluded that the polarization curve demonstrates how *M. acuminata* peduncle juice functions as a combination of cathodic and anodic inhibitors to lessen mild steel corrosion in salty settings. Electrochemical impedance spectroscopy studies show that *M. acuminata* peduncle juice prevents mild steel from corroding using active regions adsorbed onto its surface. Corrosion inhibition efficacy increases as *M. acuminata* peduncle juice concentration increases according to polarization studies. Conversely, an increase in temperature diminished the efficacy of corrosion inhibition. At 300 K with 0.3 g L^{-1} extract, the maximum corrosion inhibition is 88.0%. The Freundlich isotherm equation predicts that the physical adsorption of *M. acuminata* peduncle juice on mild steel proceeds as per a thermodynamic analysis. Temperature and concentration affect how well the MAPJ inhibits. In accordance with the values of the adsorption equilibrium constant K_{ads}, the inhibition effectiveness decreases as the temperature increases for the higher concentration, indicating that physical adsorption predominates. *M. acuminata* peduncle juice is shown to be a potent new ecologically friendly mild steel corrosion inhibitor under salty conditions according to a surface investigation.

Data availability

The author confirm that the data supporting this study's conclusions is included in the publication.

Author contributions

All contributed 100 percent to the study's development, from experimentation to analysis.

Conflicts of interest

There is no conflict of interest in this work.

Acknowledgements

The authors acknowledge the financial support through Researchers Supporting Project number (RSP2024R54), King Saud University, Riyadh, Saudi Arabia.

References

1 N. A. Barghout, A. El Nemr and B. A. Abd-El-Nabey, Use of orange peel extract as an inhibitor of stainless steel corrosion during acid washing in a multistage flash desalination plant, *J. Appl. Electrochem.*, 2023, **53**, 379–399, DOI: 10.1007/s10800-022-01772-0.

2 S. I. Ezugha and C. C. Aralu, Evaluation of adsorption and corrosion inhibition properties of *Solanum Macrocarpon* leaves extract on mild steel in sulphuric acid solutions, *SN Appl. Sci.*, 2023, **5**, 381, DOI: 10.1007/s42452-023-05594-3.

3 Y. Wu, Y. Zhang, Y. Jiang, Y. Qian, X. Guo, L. Wang and J. Zhang, Orange peel extracts as biodegradable corrosion inhibitor for magnesium alloy in NaCl solution: Experimental and theoretical studies, *J. Taiwan Inst. Chem. Eng.*, 2020, **115**, 35–46, DOI: 10.1016/j.jtice.2020.10.010.

4 N. A. Odewunmi, S. A. Umoren and Z. M. Gasem, Utilization of watermelon rind extract as a green corrosion inhibitor for mild steel in acidic media, *J. Ind. Eng. Chem.*, 2015, **21**, 239–247, DOI: 10.1016/j.jiec.2014.02.030.

5 M. Alimohammadi, M. Ghaderi, S. A. Ramazani, M. Mohammad, et al., *Falcaria vulgaris* leaves extract as an eco-friendly corrosion inhibitor for mild steel in hydrochloric acid media, *Sci. Rep.*, 2023, **13**, 3737, DOI: 10.1038/s41598-023-30571-6.

6 M. Barbouchi, B. Benzidia, A. Aouidate, A. Ghaleb, M. El Idrissi and M. Choukrad, Theoretical modeling and experimental studies of Terebinth extracts as green corrosion inhibitor for iron in 3% NaCl medium, *J. King Saud Univ., Sci.*, 2020, **32**(7), 2995–3004, DOI: 10.1016/j.jksus.2020.08.004.

7 M. A. Hossein Jafari, A. Dehghani and B. Ramezanzadeh, Investigating the effectiveness of Watermelon extract-zinc ions for steel alloy corrosion mitigation in sodium chloride solution, *J. Mol. Liq.*, 2022, **346**, 117086, DOI: 10.1016/j.molliq.2021.117086.

8 M. Ramezanzadeh, Z. Sanaei, G. Bahlakeh and B. Ramezanzadeh, Highly effective inhibition of mild steel corrosion in 3.5% NaCl solution by green Nettle leaves extract and synergistic effect of eco-friendly cerium nitrate additive: Experimental, MD simulation and QM investigations, *J. Mol. Liq.*, 2018, **256**, 67–83, DOI: 10.1016/j.molliq.2018.02.021.

9 V. Vorobyova, M. Skiba and K. Andrey, Tomato pomace extract as a novel corrosion inhibitor for the steel in industrial media: The role of chemical transformation of the extract and proinhibition effect, *J. Mol. Struct.*, 2022, **1264**, 133155, DOI: 10.1016/j.molstruc.2022.133155.

10 D. I. Njoku, C. N. Njoku, H. Lgaz, P. C. Okafor, E. E. Oguzie and Y. Li, Corrosion protection of Q235 steel in acidic-chloride media using seed extracts of Piper guineense, *J. Mol. Liq.*, 2021, **330**, 115619, DOI: 10.1016/j.molliq.2021.115619.

11 L. Xuan Bacha, D. Thi-Bich-Ngoc, K.-L. Duong-Ngoa, N. T. Thanh, T. Le Minhd, H. Nguyen Tronge, C. T. Hoang Ngoca and C. Panaitescuf, Nguyen To Hoaia,band Nam Nguyen Dang Inhibitive behaviours of unripe banana peel extract for mitigatingelectrochemical corrosion of carbon steel in aggressively acidic solutions, *J. Taibah Univ. Sci.*, 2023, **17**(1), 2247633, DOI: 10.1080/16583655.2023.2247633.

12 R. C. Purnama and A. Primadiamanti, Phytochemical screening and spectrum profile of functional group from Banana (*Musa paradisiaca* L.) stem waste extract using Fourier-transform Infrared (FTIR) Spectroscopy method, *J. Phys.: Conf. Ser.*, 2021, **1882**, 012106.

13 N. Gunavathy and S. C. Murugavel, Corrosion inhibition study of bract extract of *Musa acuminata* inflorescence on

mild steel in hydrochloric acid medium, *IOSR J. Appl. Chem.*, 2013, **5**(2), 29–35.

14 M. Balajii and S. Niju, Banana peduncle – A green and renewable heterogeneous base catalyst for biodiesel production from Ceiba pentandra oil, *Renewable Energy*, 2020, **146**, 2255–2269, DOI: **10.1016/j.renene.2019.08.062**.

15 G. Gupta, M. Baranwal, S. Saxena and M. S. Reddy, Utilization of Banana Stem Juice as a Feedstock Material for Bioethanol Production, *Clean: Soil, Air, Water*, 2019, 1900047, DOI: **10.1002/clen.201900047**.

16 N. Jyothirmayi and N. Mallikarjuna Rao, *J. Med. Sci. Technol.*, 2015, **4**(2), 152–160.

17 A. K. Niamah, Determination, Identification Of Bio Active Compounds Extracts From Yellow Banana Peels And Used *In Vitro* As Antimicrobial, *Int. J. Phytomed.*, 2014, **6**(4), 625–632.

18 Z. Zhou, X. Min, S. Wan, J. Liu, B. Liao and X. Guo, A novel green corrosion inhibitor extracted from waste feverfew root for carbon steel in H_2SO_4 solution, *Results Eng.*, 2023, **17**, 100971, DOI: **10.1016/j.rineng.2023.100971**.

19 V. Vorobyova, M. Skiba and E. Gnatko, Agri-food wastes extract as sustainable-green inhibitors corrosion of steel in sodium chloride solution: A close look at the mechanism of inhibiting action, *S. Afr. J. Chem. Eng.*, 2023, **43**, 273–295, DOI: **10.1016/j.sajce.2022.11.004**.

20 Z. Ali, E. Bahmani and A. S. Rouh Aghdam, Plant extracts as sustainable and green corrosion inhibitors for protection of ferrous metals in corrosive media: A mini review, *Corros. Commun.*, 2022, **5**, 25–38, DOI: **10.1016/j.corcom.2022.03.002**.

21 A. Dehghani, P. Ghahremani and A. H. Mostafatabar, ., Plant extracts: Probable alternatives for traditional inhibitors for controlling alloys corrosion against acidic media—A review, *Biomass Convers. Biorefin.*, 2022, **14**(4), 1–20, DOI: **10.1007/s13399-022-02893-4**.

22 Z.-G. Luo, Y. Zhang, H. Wang, S. Wan, L.-F. Song, B.-K. Liao and X.-P. Guo, Modified nano-lignin as a novel biomass-derived corrosion inhibitor for enhanced corrosion resistance of carbon steel, *Corros. Sci.*, 2024, **227**, 111705, DOI: **10.1016/j.corsci.2023.111705**.

23 V. Pourzarghan and B. Fazeli-Nasab, The use of *Robinia pseudoacacia* L fruit extract as a green corrosion inhibitor in the protection of copper-based objects, *Heritage Sci.*, 2021, **9**, 75, DOI: **10.1186/s40494-021-00545-w**.

24 C. Verma, E. E. Ebenso, I. Bahadur and M. A. Quraishi, An overview on plant extracts as environmental sustainable and green corrosion inhibitors for metals and alloys in aggressive corrosive media, *J. Mol. Liq.*, 2018, **266**, 577–590, DOI: **10.1016/j.molliq.2018.06.110**.

25 J. Kaur, N. Daksh and A. Saxena, Corrosion Inhibition Applications of Natural and Eco-Friendly Corrosion Inhibitors on Steel in the Acidic Environment: An Overview, *Arabian J. Sci. Eng.*, 2022, **47**, 57–74, DOI: **10.1007/s13369-021-05699-0**.

26 S. Banerjee, V. Srivastava and M. M. Singh, Chemically modified natural polysaccharide as green corrosion inhibitor for mild steel in acidic medium, *Corros. Sci.*, 2012, **59**, 35–41, DOI: **10.1016/j.corsci.2012.02.009**.

27 K. Azzaoui, E. Mejdoubi, S. Jodeh, A. Lamhamdi, E. Rodriguez-Castellón, M. Algarra, A. Zarrouk, A. Errich, R. Salghi and H. Lgaz, Eco friendly green inhibitor Gum Arabic (GA) for the corrosion control of mild steel in hydrochloric acid medium, *Corros. Sci.*, 2017, **129**, 70–81, DOI: **10.1016/j.corsci.2017.09.027**.

28 E. Ituen, O. Akaranta, A. James and S. Sun, Green and sustainable local biomaterials for oilfield chemicals: Griffonia simplicifolia extract as steel corrosion inhibitor in hydrochloric acid, *Sustainable Mater. Technol.*, 2017, **11**, 12–18, DOI: **10.1016/j.susmat.2016.12.001**.